Microfluidic Phenotyping of Cilia-Driven Mixing for the Assessment of Respiratory Diseases

Stephan Jonas[1,2], Engin Deniz[3], Mustafa K. Khokha[3,4], Thomas M. Deserno[1], Michael A. Choma[2,3]

[1]Department of Medical Informatics, RWTH Aachen University, Aachen, Germany
[2]Dept. Diagnostic Radiology, Yale University School of Medicine, New Haven, USA
[3]Department of Pediatrics, Yale University School of Medicine, New Haven, USA
[4]Department of Genetics, Yale University School of Medicine, New Haven, USA
stephan.jonas@yale.edu

Abstract. The function of ciliated surfaces to clear mucus from the respiratory system is important for many respiratory diseases and, therefore, has a high impact on public health. In this work, we present a quantitative method to evaluate mixing efficiency of cilia-driven microfluidic flow based on front line deformation as an integrated measurement of cilia function. So far, mixing efficiency has been used mainly for analyzing artificial cilia. Most of this work, however, was either bound to specific imaging modalities or done on simulated data. In this simulations, mixing efficiency has been quantified as the change in length of a virtual dye-strip. We adopt this measure for *in-vivo* data of the Xenopus tropicalis tadpole that is acquired by an innovative low-cost mixing assay (microscopy) and optical coherence tomography (OCT). Mixing is imaged in a water filled well while dye flows into it. The length of front line is extract with the following steps: (i) filtering of the video to reduce compression artifacts, (ii) segmentation of dye based on the hue channel in HSV colorspace, (iii) extracting and converting the front line of segmented dye to curvature scale space, and (iv) smoothing of the front line with a Gaussian filter and calculation of length in curvature scale space. Since dye cannot be used with OCT, we use data from prior work that performs particle tracking to generate a flow vector field and seed virtual dye in this flow field. The following steps extract the vector field: (i) filtering and gray scale thresholding for particle candidate detection, (ii) thresholding size of particle candidates, (iii) pairing of remaining particles from subsequent frames, (iv) estimation of velocity and direction of each particle, and (v) combining these measures into a velocity field. Our *in-vivo* imaging and analysis shows that the front line of dye is actively mixed by the ciliated surface of the Xenopus embryo.

1 Introduction

Motile cilia are organelles that protrude from the surface of cells and generate directional, low Reynolds number fluid flow. Cilia-driven flow is important for human health. For example, the respiratory system is covered with cilia that

T. Tolxdorff et al. (Hrsg.), *Bildverarbeitung für die Medizin 2012,* Informatik aktuell,
DOI 10.1007/978-3-642-28502-8_25,

clear mucus from the respiratory system. Just as artificial cilia can drive microfluidic mixing, we have preliminary data showing that biological cilia can similarly drive microfluidic mixing. Since prior work in artificial cilia has shown that mixing efficiency can be used as a measurement of ciliary function [1, 2, 3], we are interested in translating these measurements to use in biological ciliated surfaces [4]. Since quantification of mixing is bound to the imaging modality, we present a method that can be applied to data of different imaging modalities. We apply our quantitative method to images of cilia-driven fluid flow acquired using optical coherence tomography (OCT) [5] and bright field microscopy.

2 Materials and methods

Since low Reynolds number flow does not have turbulent flow to mixing, other mechanisms are required to drive efficient mixing [6]. Those mechanisms often focus on increasing fluid stirring, thereby facilitating diffusion/mixing. Therefore, the length of front line (LFL) of dye, the length of the interface between dye and water is an important factor that influences the speed of mixing by diffusion. Flow and mixing generated by the ciliated epidermis (skin) of Xenopus embryos (tadpoles) were imaged. We chose Xenopus because (i) it is genetically-manipulable [7] and (ii) it is an emerging animal model in ciliary biology [8].

A measurement similar to the one used by Khatavkar et al. (2007) was implemented to define mixing efficiency in both imaging modalities (Fig. 1). We compare the front (or dye-water interface) length of either virtual dye seeded into vector fields, or of the tracked front of dye the mixing experiments.

2.1 Optical coherence tomography

Two-dimensional two-component vector fields of cilia-driven flow were extracted using a commercially available optical coherence tomography (OCT) system (16kHz swept source OCT, Thorlabs, Inc., Newton, NJ, USA) and particle tracking of tracer particles (Fig. 1(a) and 2(a)) [5]. The particles were micro-beads with a diameter of 5μm. Images of the particles were acquired with a frame rate of 30 fps and filtered with an 3D average filter. Beads were then segmented based on one fixed gray scale threshold chosen manually for all acquisitions. A single fixed threshold is possible due to the consistency of OCT data. The segmented connected components were collected and thresholded with a size-based rejection rule to eliminate false-positives. The centroid of the particles was calculated, thus attaining sub-pixel resolution. Particles were paired based on a maximum-matching algorithm to account for particles leaving the field of view. Tracking results were combined to two-dimensional, two-component flow vector fields. In the resulting field, a line of virtual dye was seeded and the LFL of the virtual dye was calculated as a function of time. We assumed (i) that flow is low Reynolds number (i.e. $Re < 1$), (ii) that dye diffusion is slow compared to flow-mediated transport of dye, and (iii) that flow is 2D. We acknowledge that the last assumption (iii) is violated at certain points in the flow field while

highlighting that the method should be readily scaled to three-dimensional flow velocimetry.

2.2 Brightfield microscopy

The mixing assay uses bright field microscopy with a commercially available microscope (SMXZ800, Nikon Instruments, Inc, Melville, NY, USA) and camera (Mark 5 dII, Canon U.S.A., Inc, Lake Success, NY, USA) for acquisition. Dye flow imaging was performed with the ciliated embryo in a round well with inlet for dye or other flow tracers (Fig. 1(b)). Images were acquired in full HD resolution with a frame rate of 30 fps and color-normalized to account for changes in illumination by averaging the RGB channels. The original video is compressed by the camera with the H.264 codec. To reduce compression artifacts, the video is filtered with a moving average filter with kernel size 3 (Fig. 3). The dye was segmented based on the HSV colorspace. Using the hue channel, a piece of the "HSV pie" was cut out corresponding to the observed color of the dye by setting an lower and upper threshold on the hue value. Due to the color normalization, fixed thresholds for hue could be used. The front of the segmented dye was extracted by filtering the segmented image with an edge detector. It was then

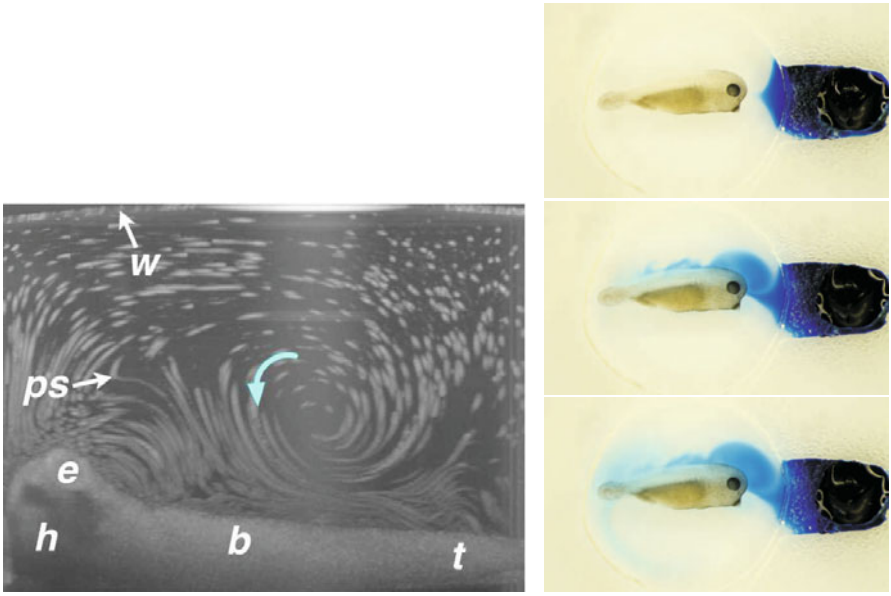

(a) OCT (b) brightfield microscopy

Fig. 1. Multi-modal source data. The projection over time of OCT images shows a water/air barrier (w), streak lines produced by the particles (ps), and the animal (eye (e), head (h), body (b) and tail (t)). The blue arrow indicates the direction of flow. In video microscopy, the blue dye is clearly visible.

converted into curvature scale space [9], addressing pixels belonging to the dye by coordinates along the front instead of a using binary mask to mark pixels as part of the dye front. The front line is then smoothed by filtering the coordinates with a Gaussian filter before the LFL was calculated.

3 Results

The data acquired by the OCT (Fig. 1(a)) visualizes the tracer particles and can be transferred into a vector field (Fig. 2(a)) by applying particle tracking [5]. Based on this field, the deformation of dye due to flow is simulated. A virtual streak of dye is seeded into the field and deformed according to the velocity field. Movement over time of the simulated dye (Fig. 4(a)) results in a change of LFL (Fig. 4(c)). In contrast for diffusing dye, the LFL is constant over the time as the gradient of the diffusion does not change on the entire front line.

The images acquired by the novel mixing assay (Fig. 1(b)) are segmented based on the hue channel of the HSV colorspace (Fig. 2(b)). The change in LFL during mixing (Fig. 4(b)) is almost linear (Fig. 4(d)), while the LFL of dye moving only by diffusion is almost constant in the observed timespan. This is according to the virtual model and proofs the applicability of this method.

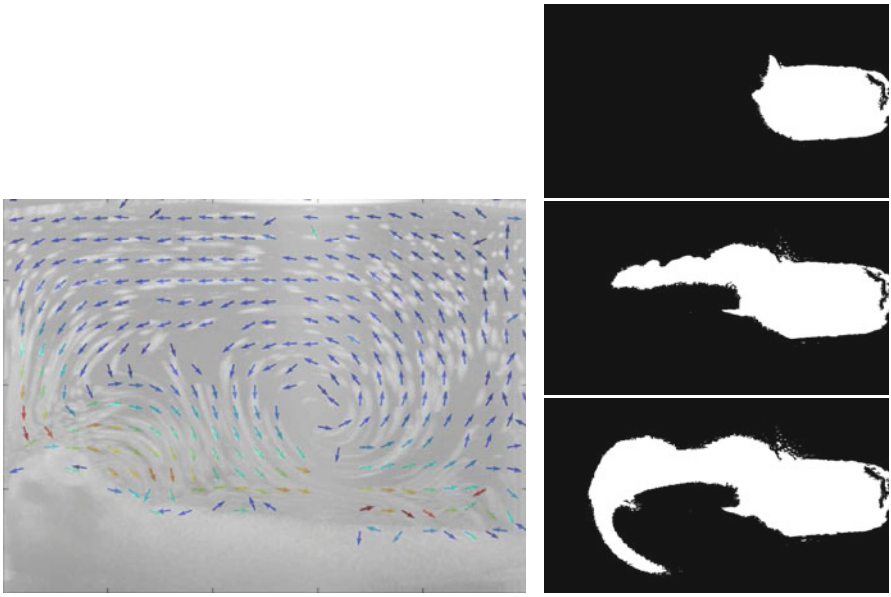

(a) OCT (b) brightfield microscopy

Fig. 2. Image processing. The velocity vector field is superimposed on Fig. 1(a) [5]. The vectors indicate direction and color indicates velocity. Velocity is scaled from blue (> 0 mm/s) to red (300 mm/s). In video microscopy, dye is segmented by static thresholding in HSV colorspace.

4 Discussion

The results indicate that the front line of dye that is actively being mixed by the ciliated surface of the Xenopus embryo at low Reynolds number flow behaves very differently from undisturbed diffusing dye. While the LFL does not change for simulated undisturbed diffusion, the LFL doubles within three seconds in case of active mixing. Similar observations can be made for the comparison of diffusion and mixing of the real dye in the low cost assay. The length of the diffusing dye only changes a few percent from the initial length, the length of the mixed dye doubles in about two minutes.

We show that by tracking the LFL of dye or simulated dye we can create a readout that can be useful to describe mixing efficiency. After assessing the robustness of our method, the next steps will be testing of gene-manipulated or pharmacologically manipulated animals. We will also investigate our measurement for its suitability for a low-cost screening assay of motile cilia with little available resources.

References

1. Khatavkar VV, Anderson PD, den Toonder JMJ, et al. Active micromixer based on artificial cilia. Phys Fluids. 2007;19:13.
2. Johnson TJ, Ross D, Locascio LE. Rapid microfluidic mixing. Anal Chem. 2002;74(1):45–51.
3. Oh K, Smith B, Devasia S, et al. Characterization of mixing performance for biomimetic silicone cilia. Microfluid Nanofluidics. 2010;9:645–55.

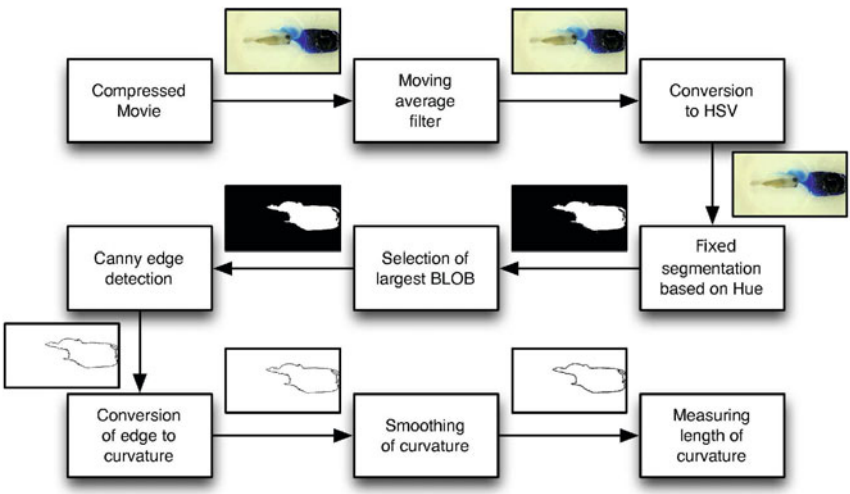

Fig. 3. Processing chain for dye mixing videos of the mixing array

4. Camesasca M, Kaufman M, Manas-Zloczower I. Quantifying fluid mixing with the Shannon entropy. Macromol Theory Simulation. 2006;15(8):595–607.
5. Jonas S, Bhattacharya D, Khokha MK, et al. Microfluidic characterization of cilia-driven fluid flow using optical coherence tomography-based particle tracking velocimetry. Biomed Opt Expr. 2011;2:2022–34.
6. Squires TM, Quake SR. Microfluidics: fluid physics at the nanoliter scale. Rev Mod Phys. 2005;77:977–1026.
7. Khokha MK, Chung C, Bustamante EL, et al. Techniques and probes for the study of Xenopus tropicalis development. Dev Dyn. 2002;225:499–510.
8. Mitchell B, Jacobs R, Li J, et al. A positive feedback mechanism governs the polarity and motion of motile cilia. Nature. 2007;447:97–101.
9. Sadegh Abbasi JK Farzin Mokhtarian. Curvature scale space image in shape similarity retrieval. Multimedia Syst. 1999;7:467–76.

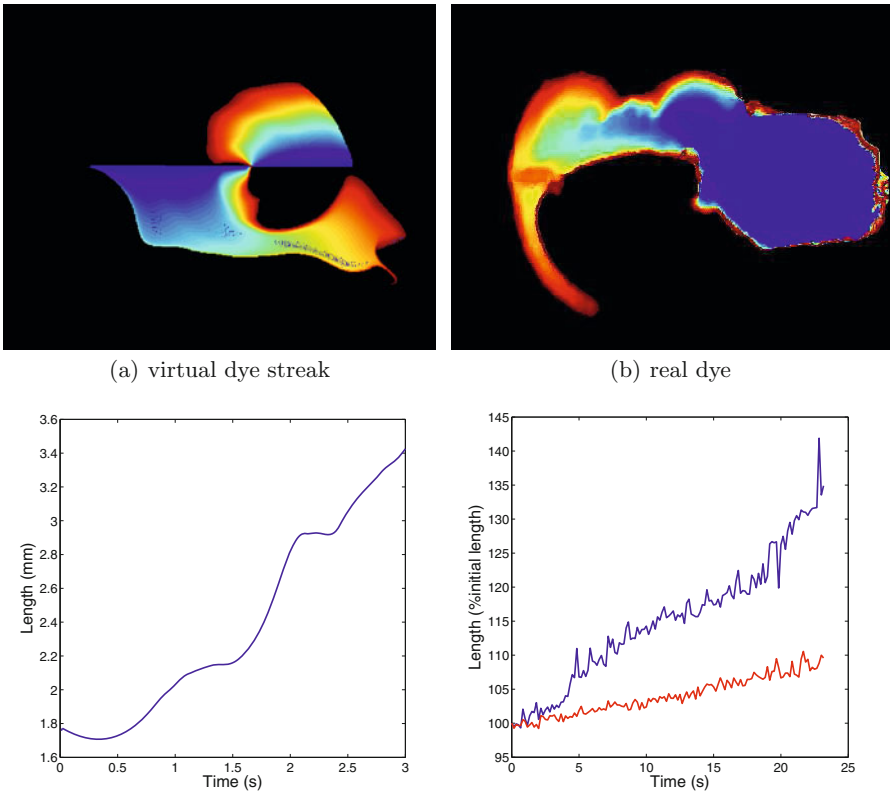

(a) virtual dye streak (b) real dye

(c) virtual dye streak (d) real dye

Fig. 4. Deformation and change in LFL of OCT data and real dye in our mixing assay. (a) and (b) show the movement of dye over the time, which is indicated from blue to red. The length (% of inital LFL) of real dye is indicated with (blue) and without active mixing (red)